

while in the deuteron potential these parameters were taken to be 6 MeV, 1.0 F, and 1.0 F, respectively. A surface-absorption term was used in the central potential for both protons and deuterons. In these calculations it was assumed that the neutron is picked up from a $p_{3/2}$ state in Be^9 . The cross section calculated using these parameters is shown in Fig. 1.

Although the calculated $\langle T_{2q} \rangle$ generally agree with the measurements in sign, they seem to be consistently smaller than the measured values by at least an order of magnitude. Varying the depth of the central potential and using volume absorption instead of surface absorption for the deuteron does not improve the agreement significantly, nor does the use of a complex spin-orbit term. The effect of increasing V_s in the deuteron potential from 6 to 8 MeV is to increase the magnitude of $\langle T_{22} \rangle$ by about a factor of 2 and to increase $\langle T_{21} \rangle$ somewhat less, but the predicted $\langle T_{20} \rangle$ then become positive for angles less than about 60° .

It remains to be seen whether the small values of the $\langle T_{2q} \rangle$ predicted by the DWBA calculations result from the failure to include additional spin-dependent inter-

actions, such as the tensor interaction, in the calculations. Another possible shortcoming of the calculations may be the assumption that Be^9 is well described by a $p_{3/2}$ neutron moving in the field of a spherically symmetric Be^8 core. The inclusion of deformation effects in the Be^9 nucleus might alter the predictions of the DWBA appreciably.

V. ACKNOWLEDGMENTS

The authors are indebted to Dr. G. R. Satchler for performing the DWBA calculations referred to in the text. In addition, we would like to express our gratitude to Dr. Louis Brown, Dr. Hans Christ and Dr. Hermann Rudin for permission to quote some of their results on the $\text{He}^3(d,p)\text{He}^4$ reaction. Thanks are also due to Dr. L. McIntyre for permission to use his results on the cross section for the $\text{He}^3(d,p)\text{He}^4$ reaction. The work of Bro. Cosmas, C.S.C. and his colleagues in constructing the scattering chamber is likewise gratefully acknowledged. Finally, the authors would like to express their gratitude to James Hevezi and George Spalek for many hours of assistance in collecting the data.

Regeneration of K_1^0 Mesons and the K_1^0 - K_2^0 Mass Difference*

J. H. CHRISTENSON,[†] J. W. CRONIN,[‡] V. L. FITCH,[‡] AND R. TURLAY[§]

Princeton University, Princeton, New Jersey

(Received 9 June 1965)

We have studied the regeneration of K_1^0 mesons using a beam of K_2^0 mesons produced at the Brookhaven AGS. The K_1^0 mesons were detected with a pair of magnet-spark-chamber spectrometers that momentum-analyzed the two decay pions. A test of the coherence of the transmission regeneration is made by comparing the yields from half- and full-density copper regenerators. The K_1^0 - K_2^0 mass difference was measured with a regenerator consisting of two pieces of copper separated by a variable air gap. This method is independent of all nuclear scattering parameters and yields a mass difference of 0.50 ± 0.10 in units of \hbar/τ_1 (where τ_1 is the K_1^0 mean life). Data taken with single copper regenerators of various thicknesses yield mass differences consistent with this measurement. Mass differences larger than 1.0 are strongly rejected by our data. The forward regeneration cross sections for C, Cu, Fe, and W were measured and found to agree with optical-model calculations. Regeneration in liquid hydrogen was also investigated and the results compared with theoretical predictions.

I. INTRODUCTION

THE striking prediction¹ that the passage of a parallel beam of K_2^0 mesons through a slab of material generates a parallel beam of K_1^0 mesons was

confirmed by R. H. Good *et al.*² The regeneration theory^{3,4} predicts a dependence of the K_1^0 intensity on the mass difference. The mass difference has been measured via the regeneration phenomenon by several authors.^{2,5} The present experiment was performed to study the coherent regeneration mechanism in detail and to make a precise measurement of the K_1^0 - K_2^0 mass difference.

* Work supported by the U. S. Office of Naval Research Contract Nonr-1858(06). This work made use of computer facilities supported in part by a National Science Foundation grant.

[†] Present address: Nevis Laboratories, Columbia University, Irvington, New York.

[‡] A. P. Sloan Foundation Fellow.

[§] Present address: Laboratoire de Physique Corpusculaire à Haute Energie, Centre d'Etudes Nucléaires, Saclay, France.

¹ A. Pais and O. Piccioni, *Phys. Rev.* **100**, 1487 (1955).

² R. H. Good, R. P. Matsen, F. Muller, O. Piccioni, W. M. Powell, H. S. White, W. B. Fowler, and R. W. Birge, *Phys. Rev.* **124**, 1223 (1961).

³ M. L. Good, *Phys. Rev.* **106**, 591 (1957).

⁴ K. M. Case, *Phys. Rev.* **103**, 1449 (1956).

⁵ T. Fujii, J. V. Jovanovich, F. Turkot, and G. T. Zorn, *Phys. Rev. Letters* **13**, 253, 324 (1964).

The propagation of a K^0 beam is described by a pair of coupled differential equations:

$$\begin{aligned} dK_2^0/dx &= AK_2^0 + BK_1^0, \\ dK_1^0/dx &= CK_1^0 + DK_2^0. \end{aligned}$$

The coefficients are the rates of change of the K_1^0 and K_2^0 amplitudes due to scattering, decay, and propagation, namely,

$$\begin{aligned} A &= 2\pi i N f_{22}(0)/k_2 + ik_2 - 1/2\Lambda_2, \\ B &= 2\pi i N f_{12}(0)/k_2, \\ C &= 2\pi i N f_{22}(0)/k_1 + ik_1 - 1/2\Lambda_1, \\ D &= 2\pi i N f_{21}(0)/k_1, \end{aligned}$$

where N is the number of nuclei per cubic centimeter, k_1 and k_2 are the wave numbers of the K_1^0 and K_2^0 , and Λ_1 and Λ_2 are their respective mean decay lengths. The regeneration amplitude is $f_{21}(0) = -f_{12}(0) = \frac{1}{2}(f_+ - f_-)$, where f_+ and f_- are the forward scattering amplitudes for the strangeness $+1$ and -1 states. Similarly, the K_2^0 scattering amplitude is $f_{22}(0) = f_{11}(0) = \frac{1}{2}(f_+ + f_-)$. We note that a CP violation does not alter the K_1^0 and K_2^0 scattering amplitudes provided CPT is conserved. The regeneration calculation is unaffected, but the states of definite mass and lifetime must now be written

$$K_1^0 = pK^0 + q\bar{K}^0,$$

and

$$K_2^0 = pK^0 - q\bar{K}^0,$$

where $|p|^2 + |q|^2 = 1$. The effects of a CP violation on the regeneration studies are small and are considered in the Appendix. For the present we assume CP invariance ($p = q$).

The differential equations can be solved in matrix form:

$$\begin{pmatrix} K_1^0(x) \\ K_2^0(x) \end{pmatrix} = \begin{pmatrix} R_{11}(x) & R_{12}(x) \\ R_{21}(x) & R_{22}(x) \end{pmatrix} \begin{pmatrix} K_1^0(0) \\ K_2^0(0) \end{pmatrix},$$

where $K_1^0(0)$ and $K_2^0(0)$ represent the initial amplitudes incident on the regenerator. The complete solution contains terms of the order of $|2\pi f_{21}(0)N\Lambda_1/k_1|^2$ which arise from the regeneration of K_2^0 's from the regenerated K_1^0 's. Since $K_2^0(0)$ is much greater than $K_1^0(0)$ for all cases in this experiment, these terms, as well as those arising from K_2^0 decay, are negligible. Dropping these terms, we find,

$$R(x) = e^{-N\sigma_T x/2} \begin{pmatrix} e^{-l/2} & \frac{2\pi i N \Lambda_1 f_{21}(0)}{k_1} \frac{(e^{-l/2} - e^{-i\delta l})}{-i\delta + \frac{1}{2}} \\ 0 & e^{-i\delta l} \end{pmatrix},$$

where $l = x/\Lambda_1$, the quantity σ_T is the total K_2^0 cross section, and δ is the K_1^0 - K_2^0 mass difference in units of \hbar/τ_1 ; τ_1 is the K_1^0 mean life.

A similar matrix serves to propagate the amplitudes

in vacuum:

$$V(x) = \begin{pmatrix} e^{-l/2} & 0 \\ 0 & e^{-i\delta l} \end{pmatrix}.$$

Applying $R(x)$ to a pure K_2^0 beam, we find the regeneration amplitude from a single regenerator of thickness $l = x/\Lambda_1$ to be

$$K_1^0(x) = \frac{2\pi i N \Lambda_1 f_{21}(0)}{k_1} \frac{(e^{-l/2} - e^{-i\delta l})}{-i\delta + \frac{1}{2}} e^{-N\sigma_T x/2} K_2^0(0).$$

Thus, the regenerated intensity is

$$I(K_1^0) = \left| \frac{2\pi N \Lambda_1 f_{21}(0)}{k_1} \right|^2 \times \frac{(1 + e^{-l} - 2e^{-l/2} \cos \delta l)}{\delta^2 + \frac{1}{4}} e^{-N\sigma_T x}. \quad (1)$$

The matrix method has great utility in the calculation of the K_1^0 intensity from regenerators compounded of many plates separated by air gaps. We will use this method to compute the regeneration for a number of situations in the course of this paper.

II. EXPERIMENTAL PROCEDURE

The experiment was performed at the Brookhaven alternating-gradient synchrotron (AGS). Thirty-BeV protons struck a 0.020-in. beryllium wire target to produce the neutral K mesons (see Fig. 1). A beam was defined at 30° to the incident proton direction by a $1.5 \times 1.5 \times 48$ -in. collimator placed at an average distance of 14.5 ft from the internal target. This first collimator was followed by an 18×36 -in. bending magnet of 512 kG in. that swept charged particles out of the beam. Gamma rays were largely removed by passing the beam through eight radiation lengths of lead placed upstream from the defining collimator and sweeping magnet. Three additional collimators along the beam, subtending solid angles greater than the first, removed those particles scattered from the defining collimator and those emanating from sources other than the internal target.

The material in which coherent regeneration was studied was placed 58 ft from the target (300 K_1^0 mean decay lengths). Each pion from the decay $K_1^0 \rightarrow \pi^+ + \pi^-$ passed through one of a pair of high-resolution magnet-spark-chamber spectrometers. Each spectrometer was built around an 18×36 -in. bending magnet placed on end so as to deflect particles in the vertical plane. Spark chambers mounted 10 in. from the magnet yoke displayed the entrance and exit paths of the particle. Each of the chambers consisted of two banks of five plates separated by a void of 12 in., thus providing a lever arm for the determination of the track angle. These plates, formed by stretching 0.001-in. aluminum foil on both sides of a $\frac{1}{2}$ -in. aluminum frame, were

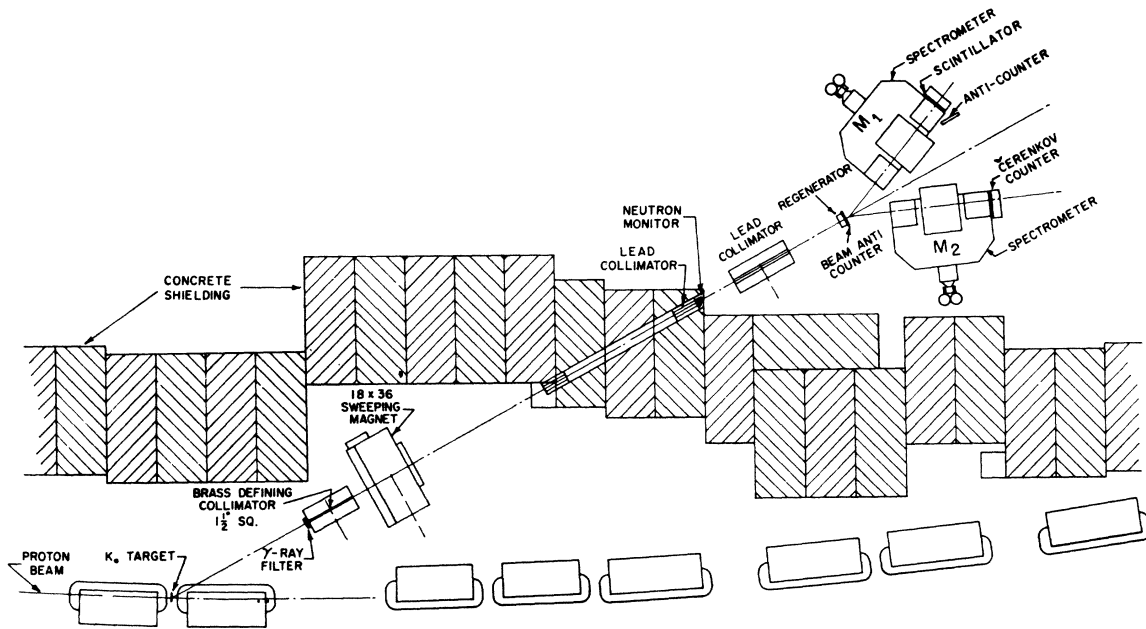


FIG. 1. Plan view of experiment. M_1 and M_2 are the spectrometer magnets.

separated by $\frac{3}{8}$ -in. gaps. Each bank presented a total of 0.008 in. of aluminum to the pions. The particles entered and left the chambers through 0.005-in. Mylar windows. A detailed description of the apparatus is given elsewhere.⁶

A scintillation counter, followed by a water Čerenkov counter, covered the exit aperture of each spectrometer. A fourfold coincidence triggered the spark chambers. A thin counter placed immediately downstream from the regenerator and operated in anticoincidence with the other counters guaranteed that the K_1^0 meson decay downstream from the anticoincidence counter. Various neutron-induced background events are thereby eliminated.

The spectrometers were placed symmetrically about the beam with an opening angle of 44° . The regenerators were placed 9 in. upstream from the vertex formed by the intersection of the spectrometer center lines. The K_1^0 mesons detected within 6 in. of the regenerator had a mean momentum of 1.1 BeV/c and a spread of ± 100 MeV/c.

The relative K_2^0 beam flux was monitored by detecting a fraction of the neutrons in the beam with a four-counter telescope placed upstream from the last collimator. An independent monitor, and one derived from the processed events directly, was provided by recording the number of three-body K_2^0 decays originating after the regenerator. This monitor was particularly suitable when the thickness of the regenerator was varied since the varying attenuation nearly cancelled out. However, these K_2^0 decays are seen in

“poor geometry” and are thus attenuated by the absorption cross section σ_A and not the total cross section σ_T .

In addition to the studies of coherent regeneration reported in this paper the apparatus was used to search for the CP -violating two-pion decays of the K_2^0 . The results of the CP experiment were reported earlier.⁷ In the entire experiment 140 000 events were recorded.

III. DATA REDUCTION

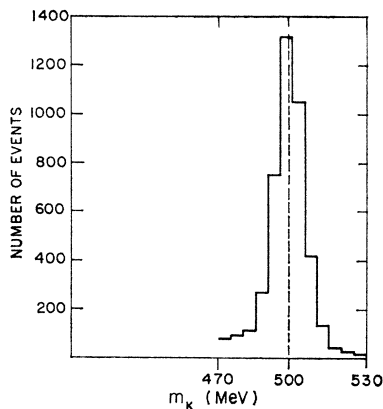
Spark-chamber photographs were scanned and measured on machines equipped with digitized angular encoders of 1.5-mrad resolution. Of all pictures taken, 35% were recognized as good events and measured by the scanners. Displacements of the tracks relative to the fiducial lines were calculated from the measured angles on the film. With the aid of measurements made on special fiducial pictures, the true space coordinates of the tracks were determined, allowing the calculation of the particle vector momenta. These momenta determined the production angle θ_K , the decay position x along the beam, and the invariant mass m_K of the two-body system, assuming both decay products to be pions. During processing, the events were subjected to a series of tests designed to ensure that both tracks emanated from a common origin and that the particles did not penetrate the magnet iron or scatter in passing through the spectrometers. A total of 67% of the measured events were successfully processed.

The events cover a mass range of 350–550 MeV, have

⁶ J. H. Christenson, A. R. Clark, and J. W. Cronin, IEEE Trans. Nucl. Sci. 11, 310 (1964).

⁷ J. H. Christenson, J. W. Cronin, V. L. Fitch, and R. Turlay, Phys. Rev. Letters 13, 138 (1964).

FIG. 2. Mass distribution for all events with $\cos\theta_K > 0.999$ and $-12 < x < -4$ in. The peak has a mean mass of 498.4 MeV and a standard deviation of 6.3 MeV.



values of $\cos\theta_K$ between 1 and 0.975 (13 deg) and decay at points along the full length of the region seen by the spectrometers, an extent of 100 in. To ascertain which of these events are coherently regenerated K_1^0 mesons, it is necessary to study the angular distribution of events whose mass m_K and decay position x are restricted to physically significant regions. A distribution of m_K for all events from solid regeneration material with $\cos\theta_K > 0.999$ and $-12 < x < -4$ in. ($x = -9$ in. is the position of the anticounter) is shown in Fig. 2. The peak is characterized by a mean mass of 498.4 MeV and a standard deviation of 6.3 MeV. A more precise analysis of a fraction of this data yields a mean mass of 498.10 ± 0.52 MeV, in good accord with the accepted value of 497.8 ± 0.6 MeV.⁸ Possible K_1^0 decays are

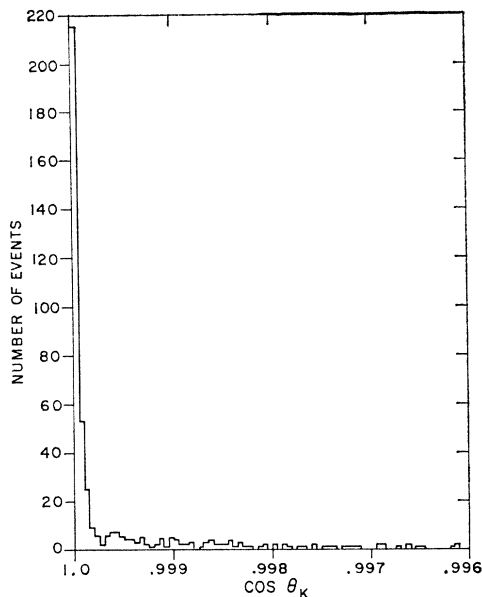


FIG. 3. Typical angular distribution of events regenerated in 3 in. of copper. The events are restricted to the range $483 < m_K < 513$ MeV and $-12 < x < -4$ in.

⁸ W. H. Barkas and A. H. Rosenfeld, University of California Radiation Laboratory Report UCRL-8030-Rev., 1963 (unpublished).

selected as those events whose masses lie in the interval 483–513 MeV and which decay within 5 in. (two K_1^0 mean decay lengths) of the regenerator.

The angular distribution of events from a 3-in. thick copper regenerator is shown in Fig. 3. The forward peak contains the transmission regenerated K_1^0 's, the forward diffraction regenerated K_1^0 's and a small K_2^0 background. The angular width of the peak is 7 mrad. This value agrees well with that found from a consideration of multiple scattering and measurement error, indicating that these K_1^0 mesons are consistent with production, precisely in the forward direction.

For small θ_K , the diffraction regeneration is Gaussian and may be written in the form

$$dN_D/d\Omega = e^{-\theta^2/2b^2} \approx e^{(\cos\theta_K - 1)/b^2}.$$

This diffraction distribution is modified by the angular response of the apparatus. Monte Carlo cal-

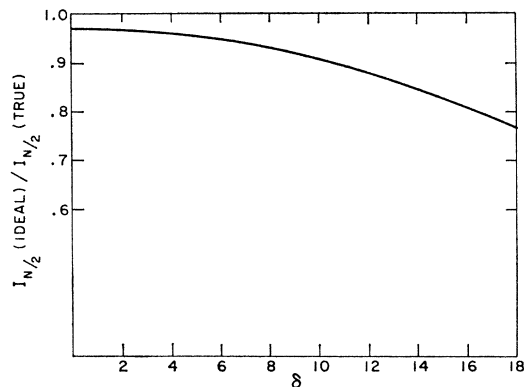


FIG. 4. Granularity correction for "half-dense" regenerator. For $\delta = 0.5$, the correction is only 3%.

culations demonstrated that the detection efficiency varies exponentially with $\cos\theta_K$, and hence the observed diffraction distribution is exponential. This background was subtracted from the forward regeneration peak by means of a maximum-likelihood fit to the data in the angular region $0.9968 < \cos\theta_K < 0.9998$. The small K_2^0 background is also exponential in $\cos\theta_K$ with a slope comparable to that of the diffraction regeneration.

IV. RESULTS

A. Comparison of Full- and Half-Density Regeneration

Equation (1) indicates that the transmission regeneration depends on the square of the density of scattering centers in the regenerator. Reducing the density of a material by one-half should diminish the K_1^0 intensity by a factor of 4. This behavior was tested by comparing regeneration from 3 in. of copper (the N regenerator) with that from a 3-in. block of "half-dense" copper ($N/2$) consisting of a stack of twelve $\frac{1}{4}$ -in.

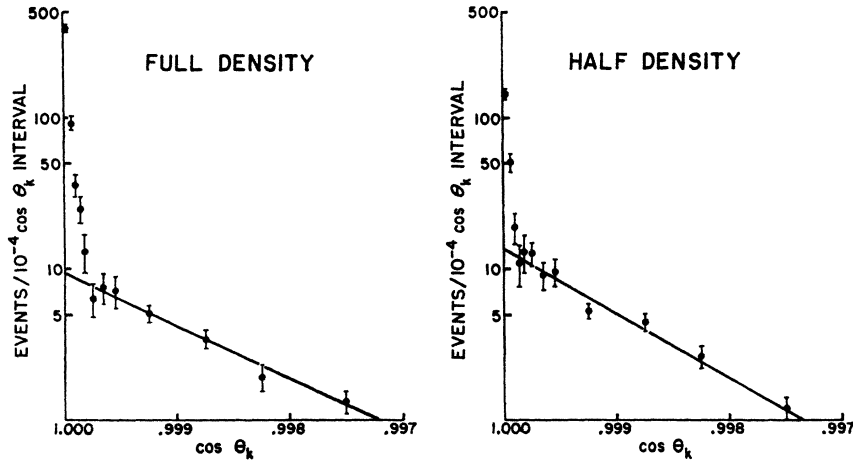


FIG. 5. Angular distributions of full- and half-density copper data. The solid line represents a maximum-likelihood fit of the function $\exp[(1 - \cos\theta_k)/b^2]$ to the diffraction regeneration.

copper plates with $\frac{1}{8}$ -in. air gaps between plates. This absorber behaves as an ideal half-density regenerator only in the limit that the granularity ($\frac{1}{8}$ in.) is negligible compared to the mass-difference wavelength Λ_1/δ . This wavelength is $4\frac{1}{2}$ in. for a mass difference of 0.5, so the granularity correction is small. In the matrix notation, the K_1^0 regeneration from the $N/2$ absorber is

$$\left| \left([R(L_0)V(L_0)]^2 \begin{bmatrix} 0 \\ 1 \end{bmatrix} \right)_1 \right|^2, \quad (2)$$

where L_0 is the individual plate thickness. The ratio of the ideal intensity as given by (1) with N replaced by $\frac{1}{2}N$ to the true intensity (2) is presented as a function of mass difference in Fig. 4. For $\delta < 2$, this ratio is seen to be very insensitive to the mass difference and equal to 0.97. The ratio S_{coh} of full- to half-density coherent regeneration is $4(0.97) = 3.88$.

If the forward regeneration were incoherent it would depend linearly on the density and S_{inc} would be about 2 (a detailed calculation yields $S_{\text{inc}} = 1.95$).

The N and $N/2$ angular distributions are presented in Fig. 5. The solid curves represent the maximum-likelihood fits to the diffraction regeneration. Multiple scattering of the regenerated K_1^0 's in the N absorber broadens the diffraction distribution, resulting in a value of b^2 larger than that of the $N/2$ data. Normalizing the data to the K_2^0 decays introduces an attenuation term into the ratio S :

$$S_{\text{expt}} = I_N/I_{N/2} |_{\text{expt}} e^{N(\sigma_T - \sigma_D)L/2} = I_N/I_{N/2} |_{\text{expt}} e^{N\sigma_D L/2},$$

where σ_D is the diffraction cross section. With a value for σ_D of 320 mb, we find $S_{\text{expt}} = 4.05 \pm 0.48$. This result is in excellent agreement with $S_{\text{coh}} = 3.88$ and is 4 standard deviations from the incoherent value $S_{\text{inc}} = 1.95$. A 20% change in σ_D alters S_{expt} by 0.14. Normalizing the data to the neutron monitor gives $S_{\text{expt}} = 4.18 \pm 0.49$ using a total cross section σ_T of 1090 mb.

B. Measurement of the Mass Difference

A large source of error in measurements of the mass difference by regeneration is the poor knowledge of the nuclear scattering parameters. We have made a measurement that is, to a high degree, devoid of any dependence on these quantities.

The regenerator used consisted of two pieces of solid copper separated by an air gap of variable width. The variation of the K_1^0 intensity with gap width depends strongly on the magnitude of the mass difference. The forward regeneration amplitude need not be known since we are interested only in the relative regeneration rate. Further, since the total amount of material in the beam is fixed, the relative intensity is independent of the total cross section σ_T .

Qualitatively, the behavior of the K_1^0 amplitude is best illustrated by the vector diagram in Fig. 6. The vector $\mathbf{a}_1(\phi)$ represents the regeneration amplitude from the upstream regenerator, while \mathbf{a}_2 is the fixed amplitude from the downstream piece. The total K_1^0 amplitude is the vector sum of the two partial amplitudes. As the gap width increases, \mathbf{a}_1 rotates about \mathbf{a}_2 and decreases in length. The total amplitude oscillates, reaching its first minimum when $\mathbf{a}_1(\phi)$ is antiparallel to \mathbf{a}_2 . The initial angle ϕ_0 is a function of the two plate thicknesses and is an odd function of the mass difference. By choosing the thicknesses properly, ϕ_0 and the initial amplitudes $\mathbf{a}_1(\phi_0)$ and \mathbf{a}_2 may be chosen to produce a null at $\phi = \pi$.

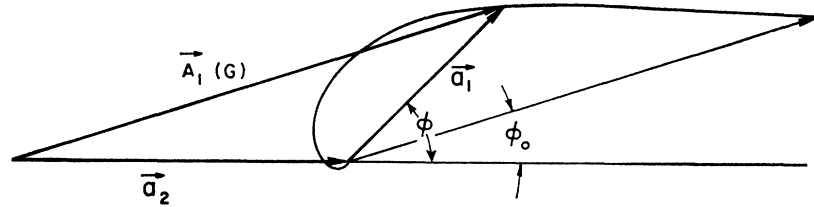
Quantitatively, the K_1^0 amplitude may be written

$$A_1(G) = \left\{ R(L_2)V(G)R(L_1) \begin{pmatrix} 0 \\ 1 \end{pmatrix} \right\}_1, \quad (3)$$

where L_1 and L_2 are the thicknesses of the two regenerator pieces. Performing the operation indicated in (3), the amplitude becomes

$$A_1(G) = a_1 e^{i\phi_1} e^{i\delta\sigma_D L/2} + a_2 e^{i\phi_2},$$

FIG. 6. Vector diagram illustrating behavior of K_1^0 amplitude as the gap width is varied.



where a_1 and a_2 are real and, together with ϕ_1 and ϕ_2 , absorb all constant factors not depending on the gap width $g = G/\Lambda_1$. The K_1^0 intensity is then

$$I_1(G) = |A_1(G)|^2 = a_1^2 e^{-g} + a_2^2 + 2a_1 a_2 e^{-g/2} \cos(\delta g + \phi_0).$$

The first term is the intensity from the upstream absorber, attenuated by K_1^0 decays across the gap. The second term is the constant intensity from the stationary downstream piece. The last term represents the interference between the two amplitudes and introduces oscillations into the otherwise exponential behavior as the gap is varied. The period of the oscillations is governed by the mass difference.

At the time of the experiment a mass difference of 1.5 to 2.0 was anticipated. By choosing $L_1 = 2$ in. and $L_2 = 1$ in., the amplitudes a_1 and a_2 and the starting phase ϕ_0 were such as to produce a minimum in the intensity for gaps of 2–3 in. The sensitivity of the shape of curves of K_1^0 intensity versus gap width to δ is demonstrated in Fig. 7.

Data were taken at seven gap widths from 0 to 3 in. and at 7 in. The data, normalized to K_2^0 decays, are presented in Fig. 8. Each point but the first represents 100–200 coherently regenerated K_1^0 's. The zero-gap point, which includes all of the data for solid 3-in. copper, includes 470 K_1^0 's. A least-squares analysis was performed to find the best values of δ . The absolute

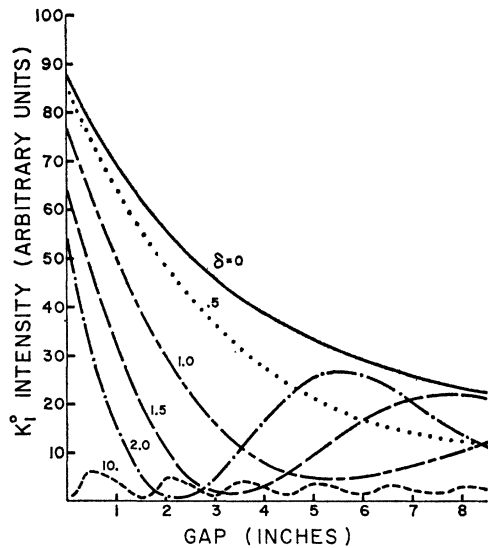


FIG. 7. Theoretical distributions of K_1^0 intensity versus gap width for various mass differences.

normalization is considered unknown and chosen to minimize χ^2 for each value of δ . The best fit to the data is achieved for $\delta = 0.47_{-0.13}^{+0.11}$. The χ^2 curve inset in Fig. 8 demonstrates the sensitivity of our data to δ . A better choice of L_1 and L_2 would render the method more sensitive to small mass differences.

The data normalized to the neutron monitor yield $\delta = 0.52 \pm 0.10$. Both values of δ are equally valid results, but are not statistically independent. Averaging the two measurements appropriately gives a final result of $\delta = 0.50 \pm 0.10$.

C. Solid-Copper Data

Additional information regarding the mass difference and validity of the regeneration theory is afforded by data taken with single solid-copper regenerators placed in the beam. The thickness of the copper was varied from 0.5 to 7.0 in. These data were analyzed in two quite different ways.

(1) Coherent Regeneration

The first method used was a direct measurement of the coherent regeneration as a function of absorber thickness. This method is the same as that used by Fujii, Jovanovich, Turkot, and Zorn.⁵ The expected relationship is that of (1). Since the material in the beam is no longer of constant thickness, an absorption correction must be made. Little experimental information is available on the total K^0 cross section σ_T , and an optical-model calculation, similar to that done by R. H. Good *et al.*,² was performed to estimate it. The K^0 and \bar{K}^0 scattering amplitudes are calculated independently and combined to yield the regeneration amplitude $f_{21}(\theta)$ and the scattering amplitude $f_{22}(\theta)$. The nuclear density function is taken to be the Fermi distribution with a nuclear radius of $1.15 A^{1/3}$ F and a falloff parameter of 0.57 F. The calculation depends on the K -nucleon forward-scattering amplitudes. The imaginary parts of these amplitudes may be determined by the total K -nucleon cross sections at 1.1 BeV/c. The cross sections used were^{9–11}: $\sigma(K^+n) = 18.0$ mb, $\sigma(K^+p) = 16.0$ mb, $\sigma(K^-n) = 37.0$ mb, and $\sigma(K^-p) = 44.5$ mb. The \bar{K}^0 potential was assumed to be completely absorptive and

⁹ V. Cook, D. Keefe, L. T. Kerth, P. G. Murphy, W. A. Wenzel, and T. F. Zipf, Phys. Rev. **129**, 2743 (1963).

¹⁰ O. Chamberlain, K. M. Crowe, D. Keefe, L. T. Kerth, A. Lemonic, Tin Maung, and T. F. Zipf, Phys. Rev. **125**, 1696 (1962).

¹¹ V. Cook, D. Keefe, L. T. Kerth, P. G. Murphy, W. A. Wenzel, and T. F. Zipf, Phys. Rev. Letters **7**, 182 (1961).

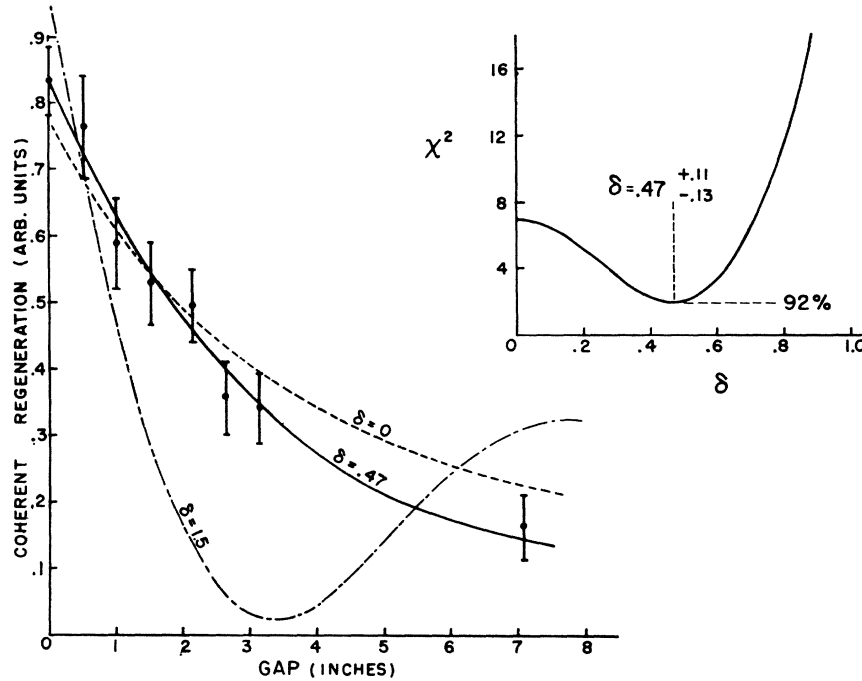


FIG. 8. Data taken with the varied-gap regenerator, normalized to the K_2^0 decays. The solid curve ($\delta=0.47$) represents the best fit to the data. All curves are normalized to minimize χ^2 . The inset curve presents χ^2 as a function of δ .

the ratio a_{R^-}/a_{I^-} of the real to imaginary forward-scattering amplitudes was zero. The corresponding ratio for the positive strangeness K^0 interaction was varied from 0 to 1. An estimate of this ratio may be made from data of Cook *et al.*⁹ on K^+p scattering. They find the real forward amplitude to be quite constant from 920 to 1970 MeV/c and equal to 0.2 ± 0.1 F in the center-of-mass system, or 0.28 ± 0.14 F in the laboratory. The imaginary part is 0.7 ± 0.3 F since the total K^+p cross section is 16.0 ± 0.6 mb. Assuming the K^+n behavior to be the same, we find $a_{R^+}/a_{I^+} = 0.44 \pm 0.20$.

Table I presents the results of the calculation for copper. The total cross section is found to be 1090 mb, in essential agreement with the recent measurement of Fujii *et al.*¹² of 985 ± 105 mb.

The regeneration data, normalized to the neutron monitor, is shown in Fig. 9. As with the gap data, a least squares analysis was done to find the best mass difference, considering the over-all normalization un-

TABLE I. Optical-model calculations for copper. The forward-scattering cross section is $|f_{22}(0)|^2$ and the forward regeneration cross section is $|f_{21}(0)|^2$. All cross sections are given in barns.

a_{R^+}/a_{I^+}	$ f_{21}(0) ^2$	$ f_{22}(0) ^2$	σ_D	σ_T
0.0	1.59	22.9	0.307	1.077
0.3	1.64	23.4	0.317	1.084
0.44	1.71	23.9	0.324	1.093
0.5	1.75	24.2	0.329	1.098
1.0	2.19	27.9	0.384	1.157

¹² T. Fujii, J. V. Jovanovich, F. Turkot, G. T. Zorn, and M. Deusch, *Proceedings of the Twelfth Annual International Conference on High-Energy Physics, Dubna, 1964* (Atomizdat, Moscow, 1965).

known. We find $\delta = 0.69 \pm 0.20$, statistically compatible with the gap measurement. The mass difference varies from 0.60 to 0.71 when σ_T is changed from 1075 to 1160 mb ($0 < a_{R^+}/a_{I^+} < 1$). An analysis of the same data normalized to the K_2^0 decays involves the diffraction cross section σ_D . Using $\sigma_D = 320$ mb, we find $\delta = 0.76 \pm 0.20$. Varying σ_D from 305 to 385 mb changes δ from 0.69 to 0.78.

(2) Ratio Analysis

A second method of treating the data, due to M. L. Good,³ involves the ratio R of coherent regeneration to diffraction regeneration per unit solid angle in the for-

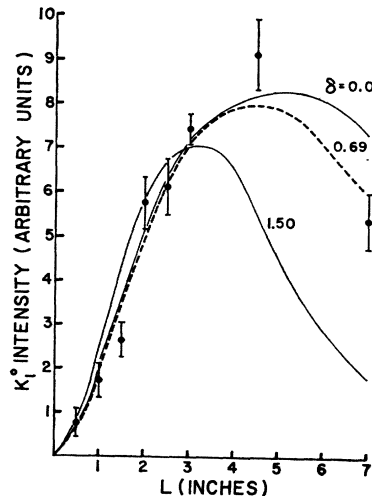


FIG. 9. Measured K_1^0 intensity versus regenerator thickness L . The data is normalized to the neutron monitor using a total cross section $\sigma_T = 1100$ mb. The dashed curve ($\delta = 0.69$) represents the best fit to the data.

ward direction:

$$R = \frac{4\pi^2 N \Lambda_1 (1 + e^{-l} - 2e^{-l/2} \cos \delta l)}{k_1^2 (\delta^2 + \frac{1}{4})(1 - e^{-l})}. \quad (4)$$

An apparent virtue of this procedure is that R involves no nuclear scattering parameters such as $|f_{21}(0)|^2$ or σ_T and is independent of the incident K_2^0 flux, so no relative normalization of the data is necessary. But, for practical regenerator thicknesss, scattering of the coherent K_1^0 wave and multiple scattering of the incoherent waves affect the diffraction regeneration noticeably. Data taken with thicknesss that provide a reasonable sensitivity to the mass difference also require large corrections. These multiple effects, discussed at length by R. H. Good *et al.*,² depend on the nuclear parameters and thus complicate the simple expression (4). The ratio of the true diffraction to that obtained by ignoring multiple effects is plotted as a function of absorber thickness in Fig. 10. The scattering amplitudes and cross sections were supplied by the optical-model calculation. This ratio is as small as 0.62 for 3 in. of copper and rises again as the thickness is further increased.

The amount of forward diffraction regeneration is determined by the background extrapolated to the $\cos \theta_K = 1$ axis. The K_2^0 background included is not negligible and must be removed. The size of the background was determined from data taken with no regenerator in the beam. The K_2^0 background removal alters the 7-in. point by 29% and increases its error from 36 to 46%. The final data are shown in Fig. 11. A least-squares analysis of the data yields $\delta = 0.41_{-0.20}^{+0.25}$. In this method the normalization is fixed and only the mass difference is varied to minimize χ^2 . Varying a_R^+/a_T^+ from 0.0 to 1.0 changes δ from 0.44 to 0.33. It is apparent from Fig. 11 that the measured value of the mass difference depends greatly

FIG. 10. Multiple-scattering correction to forward-diffraction regeneration. The ratio of the true value to that neglecting multiple scattering is plotted as a function of regenerator thickness L .

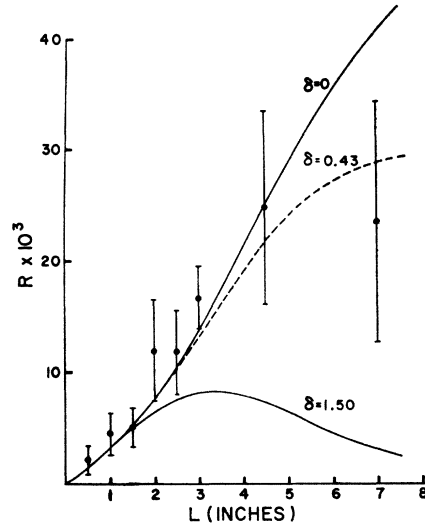
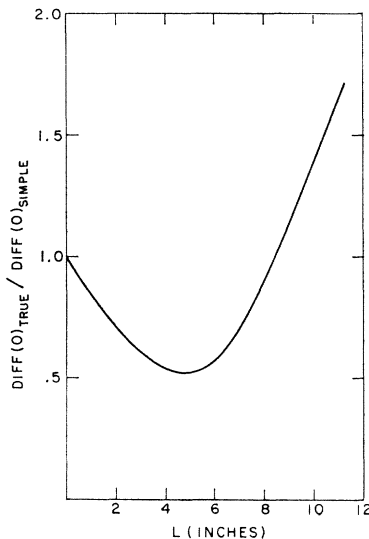


FIG. 11. Experimental ratio of coherent regeneration to forward-diffraction regeneration plotted as a function of regenerator thickness L . The dashed curve for $\delta = 0.43$ is the best χ^2 fit.

on the 7-in. point. Had δ been nearer 1.5, the data at smaller thicknesss would have played a more significant role. On the other hand, added support for the regeneration mechanism comes from the excellent agreement of the 0.5-, 1.0-, and 1.5-in. points with the predicted values of R . By expanding R to second order in l , it can be shown that R is independent of δ , provided $l \ll 1/\delta = 2$. However, the multiple scattering correction is not negligible, as seen in Fig. 10. Hence, the agreement supports both the coherent-regeneration mechanism and the multiple-scattering theory, regardless of the precise value of the mass difference.

D. Forward Regeneration Cross Sections and the K_2^0 Flux

To complete the analysis of the regeneration mechanism the absolute K_1^0 regeneration rate was calculated. All analyses of the data to this point have either been independent of the absolute normalization or this normalization has been considered unknown and varied to fit the data. Since the forward cross section $|f_{21}(0)|^2$ is not known, the absolute regeneration rate was studied by calculating $|f_{21}(0)|^2$ from data taken with various materials and comparing the results with optical-model predictions.

The K_2^0 flux was determined from data on three-body K_2^0 decays with no regenerator and no anticoincidence counter present. A total of 5035 leptonic K_2^0 decays were detected.⁷ The three-pion decays produced a well-defined peak in the two-body mass distribution one pion mass below the K_1^0 mass and have been removed. The detection efficiency of the apparatus for K_{e3} and $K_{\mu 3}$ decays was determined by a Monte Carlo calculation. The efficiencies, when coupled with the measured

TABLE II. Forward regeneration cross sections for carbon, iron, copper, and Hevimet. All cross sections are in barns. The mass difference used is 0.5.

Material	σ_T	$ f_{21}(0) ^2_{\text{theory}}$			$ f_{21}(0) ^2_{\text{expt}}$
		$a_{R^+}/a_{I^+}=0.0$	0.44	1.0	
Carbon	0.273	0.17	0.19	0.25	0.14 ± 0.04
Iron	0.970	1.34	1.45	1.88	1.10 ± 0.28
Copper	1.080	1.59	1.71	2.19	1.06 ± 0.27
Hevimet	2.430	4.73	4.96	5.85	3.74 ± 0.94

K_{e3} and $K_{\mu 3}$ branching ratios,¹³ yield a corrected total of 2.32×10^8 K_2^0 decays over a 2.5-m decay path in a momentum interval from 600 to 1800 MeV/c. The total K_2^0 beam flux at the position normally occupied by the regenerator is 2.92×10^9 (a K_2^0 lifetime of 5.3×10^{-8} sec was used¹²). The K_2^0 flux, extrapolated back to the point of production by correcting for decay along the 18.6-m path length and for absorption in the lead γ -ray filter, is 3.2×10^8 K_2^0 's/(10^{11} p-(BeV/c)-sr) at 1 BeV/c. Surveys have been made of the flux of charged K mesons at 30° at the AGS.¹⁴ Assuming the K^0 and \bar{K}^0 rates are the same as the K^+ and K^- rates at high energies, we obtain from this data a K_2^0 flux of 2.1×10^8 /(10^{11} p-(BeV/c)-sr). This number agrees, within the statistical accuracy, with our result.

The total number of K_1^0 mesons regenerated in a particular run was calculated from the observed number of K_1^0 decays, utilizing the measured detection efficiency. Values of $|f_{21}(0)|^2$ obtained in this manner from data on 3.5 in. of carbon, 1 in. of iron, 3 in. of copper and 2.125 in. of Hevimet are presented in Table II. The prime sources of error are the estimate of the true K_2^0 flux and the statistics of the K_1^0 decays. Total cross sections were obtained from the optical-model calculation. A mass difference of 0.5 was used. These

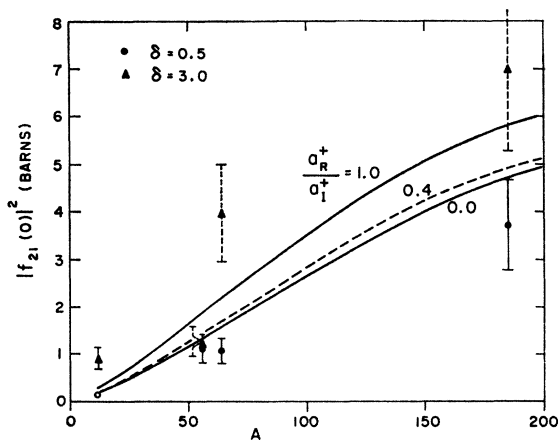


FIG. 12. Forward regeneration cross section as a function of regenerator atomic weight A . The curves represent optical-model calculations; the dashed curve is preferred.

¹³ D. Lüers, I. S. Mitra, W. J. Willis, and S. S. Yamamoto, Phys. Rev. **133**, B1276 (1964).

¹⁴ A. Schwarzschild and Č. Zupančič, Phys. Rev. **129**, 854 (1963).

forward cross sections are compared to optical-model calculations in Fig. 12. The good agreement of the data with the predicted values indicates that the expression for coherent regeneration is correct and the regeneration rates may be accounted for by conventional scattering amplitudes.

The calculation was also done for a mass difference of 3.0. The iron cross section is insensitive to δ since the regenerator was thin while the copper cross section changes by a factor of 4. The monotonic rise of $|f_{21}(0)|^2$ with A is destroyed by the assumption of large mass differences.

E. Coherent Regeneration in Hydrogen

We have placed a liquid-hydrogen target in the K_2^0 beam to measure the coherent regeneration in hydrogen. The target, 6 in. in diameter and 4 ft in length, was placed with its center at the intersection of the two spectrometers. The walls parallel to the beam direction were 0.07 gm/cm² thick. A 1.25-in.-diam. collimator replaced the normal 1.5×1.5-in. beam-defining collimator so that all of the beam passed through the target and did not strike the walls.

To compare the regeneration in hydrogen to that in heavy materials, a 2-in.-thick tungsten regenerator was placed at five positions along the 4-ft length of the target volume. The response of the apparatus, as determined from Monte Carlo calculations, varies sufficiently smoothly over the length of the target that the sum of events obtained from the five regenerator positions can be considered as if they came from a continuous distribution over the target. Thus the total detection efficiency E for the tungsten data is the same as for the hydrogen data, to a good approximation.

Since the hydrogen target length L_H is much greater than the K_1^0 mean decay length and much less than the absorption length, the equilibrium yield may be written

$$Y_H = \frac{E |2\pi N_H \Lambda_1 f_{21}^H(0)_{\text{eff}}|^2}{k_1^2 (\delta^2 + \frac{1}{4})} \times \frac{L_H}{\Lambda_1}.$$

The symbol $f_{21}^H(0)_{\text{eff}}$ is used to denote that the measured quantity is the coherent sum of the regenerated two-pion decays and the direct two-pion decays of the K_2^0 .⁷ All quantities are to be taken as appropriate averages over the momentum spectrum of the K_2^0 beam which was centered at 1.0 BeV/c, but extended from 0.7 to 1.4 BeV/c. Inserting all the appropriate numerical factors, we find for the relative tungsten and hydrogen amplitudes,

$$|f_{21}^H(0)_{\text{eff}}|^2 / |f_{21}^W(0)|^2 = 0.14 Y_H / Y_W.$$

The results of the hydrogen run are presented in Fig. 13. The sharp forward peak indicating the two-pion decays is clearly evident. These events were measured with high precision to give maximum resolution. The mass and angular resolution are somewhat poorer than

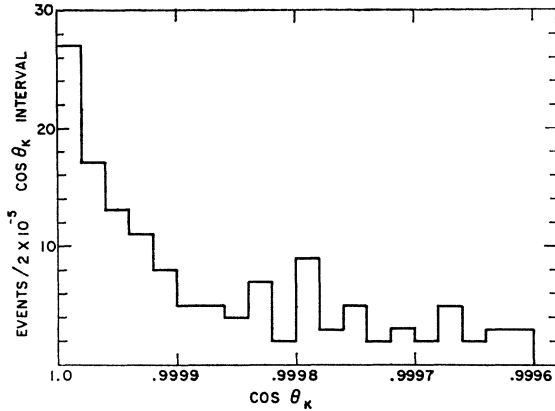


FIG. 13. Angular distribution of hydrogen events in the mass range $488 < m_K < 508$ MeV.

those obtained from the direct K_2^0 decays because of the multiple scattering encountered in the hydrogen. The background under the peak is again evaluated by extrapolation of the angular distribution to zero angle. Subtracting the background gives 48 ± 10 events for 1213 monitor counts.

The total number of events found with the tungsten regenerator was 144 ± 13 for a total of 507 monitor counts. Normalizing the two yields one finds the ratio

$$|f_{21}^H(0)_{\text{eff}}|^2 / |f_{21}^W(0)|^2 = (2.0 \pm 0.5) \times 10^{-3}.$$

Using the experimental result for the tungsten amplitude (Table II), we find

$$|f_{21}^H(0)_{\text{eff}}| = (0.85 \pm 0.15) F.$$

The total two-pion decay-intensity-per-unit-length along the target is given by

$$(\epsilon + \alpha)^2 / \Lambda_1 \equiv |\alpha_{\text{eff}}|^2 / \Lambda_1,$$

where

$$\alpha \equiv \frac{2\pi N \Lambda_1 f_{21}^H(0)}{k_1(\delta + i/2)}, \quad \alpha_{\text{eff}} = \frac{2\pi N \Lambda_1 f_{21}^H(0)_{\text{eff}}}{k_1(\delta + i/2)},$$

and ϵ is the amplitude for the direct decay of the K_2^0 to two pions. Experiment gives $|\epsilon| = (2.3 \pm 0.4) \times 10^{-3}$.⁷ The transient effects at the entrance to the target are negligible. Using our results for hydrogen, we find $|\alpha_{\text{eff}}| = (3.9 \pm 0.7) \times 10^{-3}$.

An unknown phase between ϵ and α requires that we write

$$|\alpha_{\text{eff}}|^2 = |\epsilon|^2 + |\alpha|^2 + 2|\alpha||\epsilon| \cos \phi.$$

Thus α lies in the interval $1.6 \pm 0.8 < \alpha < 7.2 \pm 0.8$ which implies $(0.35 \pm 0.18) F < f_{21}^H(0) < (1.6 \pm 0.2) F$.

These limits are to be compared with the value of $(0.50 \pm 0.06) F$ measured by Leipuner *et al.*¹⁵ directly from the process $K_2^0 + p \rightarrow K_1^0 + p$. [Note that all values of $f_{21}^H(0)$ are given in the laboratory system.]

¹⁵ L. B. Leipuner, W. Chinowsky, R. Crittenden, R. Adair, B. Musgrave, and F. T. Shively, *Phys. Rev.* **132**, 2284 (1963).

Because of the interference between the direct two-pion decays it is difficult to measure the hydrogen regeneration amplitude precisely.¹⁶ The range of values between the two limits is consistent with reasonable amplitudes. We see no evidence for anomalous regeneration of K_1^0 's in hydrogen as reported by Leipuner *et al.*¹⁵ To agree with the experimental results of Leipuner *et al.* we would need ~ 20 times the number of two-pion decays.

V. CONCLUSIONS

All data from the experiment find explanation in, and are entirely consistent with, conventional regeneration theory. A comparison between full- and half-dense regenerators has demonstrated, independent of the magnitude of the mass difference, that the transmission regeneration is coherent. The mass difference is found to be 0.50 ± 0.10 (in units of \hbar/τ_1) using two absorbers separated by an air gap. The χ^2 probability for the fit to $\delta = 0.5$ is 92%. We emphasize that this measurement does not involve any nuclear scattering parameters or corrections to the data. Regeneration of K_1^0 's in absorbers of various thicknesses yielded values of the mass difference in agreement with the more precise gap measurement, when analyzed in two independent ways. The fact that three quite different approaches to the measurement of the mass difference from K_1^0 regeneration gives essentially the same result implies a good understanding of the mechanism involved. All data strongly reject mass differences greater than 1.0. The regeneration is seen to arise from conventional scattering amplitudes and does not depend on any other intrinsic physical properties of the regenerator.

ACKNOWLEDGMENTS

The full cooperation of all members of the AGS staff during the course of the experiment is greatly appreciated. Many members of the Elementary Particles Laboratory and the Physics Department of Princeton University contributed to the success of this experiment. The analysis made extensive use of the facilities of the Princeton University Computer center. Special thanks are due to Dr. Alan R. Clark for his participation in the construction of the apparatus and the setting up of the experiment.

APPENDIX: EFFECT OF A CP VIOLATION ON THE MASS-DIFFERENCE MEASUREMENT

With CP violation implied by the observation of the two-pion decay of the K_2^0 , it is of interest to calculate its effect on the measurement of the mass difference.

¹⁶ We have spoken as if the two-pion decay of the K_2^0 was coherent with the two-pion decay of the regenerated K_1^0 . This in no way implies, however, that this experiment demonstrates an interference between the two decays.

Provided the *CPT* theorem is valid, the states of definite mass and lifetime may be written

$$\begin{aligned} K_s^0 &= pK^0 + q\bar{K}^0, \\ K_l^0 &= pK^0 - q\bar{K}^0, \end{aligned} \quad (5)$$

where $|p|^2 + |q|^2 = 1$.¹⁷ The regeneration of K_s^0 's is independent of p and q .³ This is easily seen by considering the scattering of a K_l^0 in a nuclear medium. The scattered wave function is

$$\Psi_{sc} = pf_+K^0 - qf_- \bar{K}^0,$$

where f_+ and f_- are the usual scattering amplitudes. From (5) we see that $K^0 = (K_s^0 + K_l^0)/2p$ and $\bar{K}^0 = (K_s^0 - K_l^0)/2q$. Hence Ψ_{sc} becomes

$$\begin{aligned} \Psi_{sc} &= pf_+(K_s^0 + K_l^0)/2p - qf_-(K_s^0 - K_l^0)/2q \\ &= \frac{1}{2}(f_+ - f_-)K_s^0 + \frac{1}{2}(f_+ + f_-)K_l^0 = f_{21}K_s^0 + f_{22}K_l^0, \end{aligned}$$

as usual. The regeneration calculations are thus unaffected but the K_s^0 and K_l^0 are now given by (5). Since the apparent violation is very small, we write

$$\begin{aligned} K_s^0 &= K_1^0 + \epsilon K_2^0, \\ K_l^0 &= \epsilon K_1^0 + K_2^0, \end{aligned}$$

where K_1^0 and K_2^0 are pure eigenstates of *CP* and ϵ is the *CP*-violating amplitude.

At a distance x downstream from a regenerator, the K_s^0 and K_l^0 amplitudes are

$$\begin{aligned} A_s(x) &= A_s(0)(K_1^0 + \epsilon K_2^0)e^{ik_1x}e^{-x/2\Delta_1}, \\ A_l(x) &= A_l(0)(\epsilon K_1^0 + K_2^0)e^{ik_2x}, \end{aligned}$$

where the K_l^0 lifetime is considered infinite.

The two-pion amplitude is proportional to the total K_1^0 component:

$$\begin{aligned} A_{2\pi}(x) &= A_s(0)e^{ik_1x}e^{-x/2\Delta_1} + \epsilon A_l(0)e^{ik_2x} \\ &= e^{ik_1x}(A_s(0)e^{-x/2\Delta_1} + \epsilon A_l(0)e^{i\delta x/\Lambda_1}). \end{aligned}$$

Hence the two-pion intensity at x is

$$I_{2\pi}(x) = |A_s(0)|^2 e^{-x} + |\epsilon A_l(0)|^2 + 2 \operatorname{Re} A_s^*(0) A_l(0) \epsilon e^{-x/2} e^{i\delta x}, \quad (6)$$

where x is now in units of the K_s^0 mean decay length. The first term is the normal regenerated intensity, decaying with the K_s^0 lifetime. The second term, the $K_l^0 \rightarrow 2\pi$ intensity, is small compared with the first term. The last term represents the interference between the two sources of two-pion decays and diminishes at half the K_s^0 rate.

¹⁷ T. D. Lee, R. Oehme, and C. N. Yang, Phys. Rev. **106**, 340 (1957).

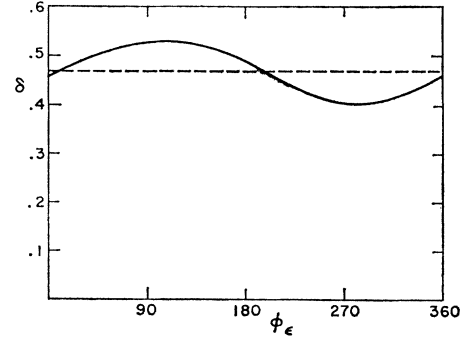


FIG. 14. Mass difference as a function of the phase of the *CP*-violating amplitude. The dashed line represents the value obtained assuming *CP* invariance.

Equation (6), integrated over the 5-in. decay region downstream from the regenerator, yields the total observed two-pion intensity.

Letting $\epsilon = |\epsilon|e^{i\phi_\epsilon}$, where ϕ_ϵ represents the sum of the phases of ϵ and $f_{21}(0)$, and $D = 5 \text{ in.}/\Lambda_1$, the intensity is

$$\begin{aligned} I_{2\pi} &= \int_0^D I_{2\pi}(x) \Lambda_1 dx \\ &= \Lambda_1 |A_s(0)|^2 (1 - e^{-D}) + |\epsilon|^2 |A_l(0)|^2 \Lambda_1 D \\ &\quad + (\Lambda_1 F_1 / (\delta^2 + \frac{1}{4})) [e^{-D/2} (\delta \sin \delta D - \frac{1}{2} \cos \delta D) + \frac{1}{2}] \\ &\quad - (\Lambda_1 F_2 / (\delta^2 + \frac{1}{4})) [\delta - e^{-D/2} (\delta \cos \delta D + \frac{1}{2} \sin \delta D)], \end{aligned} \quad (7)$$

where

$$F_1 = 2|\epsilon| \{ \cos \phi_\epsilon \operatorname{Re}[A_s^*(0) A_l(0)] - \sin \phi_\epsilon \operatorname{Im}[A_s^*(0) A_l(0)] \},$$

and

$$F_2 = 2|\epsilon| \{ \sin \phi_\epsilon \operatorname{Re}[A_s^*(0) A_l(0)] + \cos \phi_\epsilon \operatorname{Im}[A_s^*(0) A_l(0)] \}.$$

The magnitude of ϵ is $(2.3 \pm 0.4) \times 10^{-3}$, but the phase ϕ_ϵ is unknown.⁷

The gap data normalized to the K_l^0 decays was re-analyzed using (7) to compute the two-pion intensity. A least-squares fit to the data was performed to find the best values of δ for a given phase ϕ_ϵ . The results are presented in Fig. 14. The mass difference is seen to vary from 0.41 to 0.53, a variation comparable to the uncertainty in the earlier determination of the mass difference that neglected the effects of a *CP* violation ($\epsilon = 0$). The average mass difference with $\epsilon \neq 0$ is seen to be the same as that measured with $\epsilon = 0$. The data yield no information as to a preferred phase ϕ_ϵ .